Creating and exploring carboxymethyl cellulose aerogels as drug delivery devices

Sujie Yu, Tatiana Budtova

▶ **To cite this version:**

Sujie Yu, Tatiana Budtova. Creating and exploring carboxymethyl cellulose aerogels as drug delivery devices. Carbohydrate Polymers, 2024, 332, pp.121925. 10.1016/j.carbpol.2024.121925 . hal-04465349

HAL Id: hal-04465349
https://hal.science/hal-04465349

Submitted on 19 Feb 2024

HAL is a multi-disciplinary open access archive for the deposit and dissemination of scientific research documents, whether they are published or not. The documents may come from teaching and research institutions in France or abroad, or from public or private research centers.

L'archive ouverte pluridisciplinaire **HAL**, est destinée au dépôt et à la diffusion de documents scientifiques de niveau recherche, publiés ou non, émanant des établissements d'enseignement et de recherche français ou étrangers, des laboratoires publics ou privés.

Carbohydrate Polymers 332 (2024) 121925

Contents lists available at ScienceDirect

Carbohydrate Polymers

journal homepage: www.elsevier.com/locate/carbpol

Creating and exploring carboxymethyl cellulose aerogels as drug delivery devices

Sujie Yu, Tatiana Budtova *

Mines Paris, PSL University, Center for Materials Forming (CEMEF), UMR CNRS 7635, CS 10207, Rue Claude Daunesse, 06904 Sophia Antipolis, France

ARTICLE INFO

Keywords:
CMC
Density
Porosity
Release
Diffusion

ABSTRACT

Carboxymethyl cellulose (CMC) is a well-known cellulose derivative used in biomedical applications due to its biocompatibility and biodegradability. In this work, novel porous CMC materials, aerogels, were prepared and tested as a drug delivery device. CMC aerogels were made from CMC solutions, followed by non-solvent induced phase separation and drying with supercritical CO_2. The influence of CMC characteristics and of processing conditions on aerogels' density, specific surface area, morphology and drug release properties were investigated. Freeze-drying of CMC solutions was also used as an alternative process to compare the properties of the as-obtained "cryogels" with those of aerogels. Aerogels were nanostructured materials with bulk density below 0.25 g/cm^3 and high specific surface area up to 143 m^2/g. Freeze drying yields highly macroporous materials with low specific surface areas (around 5–18 m^2/g) and very low density, 0.01 - 0.07g/cm^3. Swelling and dissolution of aerogels and cryogels in water and in a simulated wound exudate (SWE) were evaluated. The drug was loaded in aerogels and cryogels, and release kinetics in SWE was investigated. Drug diffusion coefficients were correlated with material solubility, morphology, density, degree of substitution and drying methods, demonstrating tuneability of new materials' properties in view of their use as delivery matrices.

1. Introduction

Polysaccharides, the bio-based polymers derived from nature, are "human-friendly" as many are biocompatible and biodegradable and thus are widely used for food, feed, cosmetic and biomedical applications. They are very promising for replacing fossil-based polymers, and for making high value-added materials (Budtova, 2019; Seddiqi et al., 2021; Yahya, Alzalouk, Alfallous, & Abogmaza, 2020). They can be of high specific strength, possess a hierarchical structure and can be functionalised. In particular, biodegradable, bioabsorbable and bioresorbable polysaccharides offer promising possibilities for innovative delivery devices in gene therapy, cosmetics, healthcare, environmental protection, *etc.*

Cellulose is the most abundant polysaccharide. It is possible to make cellulose materials of various porosity and interconnectivity according to the needs of biomedical applications (Barclay, Day, Petrovsky, & Garg, 2019). One option is to use nanocellulose, and bacterial cellulose is already applied in medicine and cosmetics (Mbituyimana et al., 2021; Rothe et al., 2022). The other option is to perform cellulose shaping *via* dissolution, however, this pathway has certain limitations as the majority of cellulose solvents are not suitable for life science applications. Therefore, cellulose is often chemically modified to make it water-soluble. For example, carboxymethyl cellulose (CMC) is a linear, anionic, water-soluble cellulose ether, having good compatibility with skin and mucous membranes, and thus is widely used in biomedical, pharmaceutical, cosmetic and food industries (Buhus, Peptu, Popa, & Desbrières, 2009). The degree of substitution (DS) of CMC used in the biomedical field is usually between 0.6 and 1.25 (Liu, Zhai, Li, Peng, & Wu, 2002).

Many biomedical materials require porous morphology which should correspond to the selected application, for example, to support cell growth and bioactivity, facilitating nutrient delivery and oxygen transport, or for the absorption of exudates, or for controlled drug delivery. Porous CMC materials, like hydrogels and sponges, have been used in drug delivery, tissue engineering and wound dressing applications (Kanikireddy, Varaprasad, Jayaramudu, Karthikeyan, & Sadiku, 2020; Liu et al., 2002; Sadeghi, Nourmohammadi, Ghaee, & Soleimani, 2020). In most cases, CMC is crosslinked and/or mixed with other substances, such as gelatine, starch, polyvinyl alcohol, chitosan, *etc*, and used in hydrogel form (Kanikireddy et al., 2020). Few works report on

* Corresponding author.
E-mail address: Tatiana.Budtova@minesparis.psl.eu (T. Budtova).

https://doi.org/10.1016/j.carbpol.2024.121925
Received 25 November 2023; Received in revised form 16 January 2024; Accepted 5 February 2024
Available online 9 February 2024
0144-8617/© 2024 The Authors. Published by Elsevier Ltd. This is an open access article under the CC BY-NC-ND license (http://creativecommons.org/licenses/by-nc-nd/4.0/).

CMC freeze-dried materials, crosslinked (for example, with $FeCl_3$ and D-gluconic acid-δ-lactone used as releasing agent, Lin, Li, Lu, & Cao, 2015) or mixed (for example, with carbon nanotubes, Long, Li, Shu, Zhang, & Weng, 2019). Citric acid was used as cross-linker to prepare CMC and poly(ethylene oxide) hydrogel with high loading percentage of methylene blue to be potentially used for controlled drug release (Kanafi, Rahman, & Rosdi, 2019). Freeze-dried CMC/sericin cross-linked with glutaraldehyde and aluminium chloride with 3D cell-interactive environment was fabricated for tissue engineering applications (Nayak & Kundu, 2014). Sponges with interconnected pores, based on CMC/keratin, showed a significantly inhibited growth of *S. aureus* bacterial colonies after 1 day (Sadeghi et al., 2020).

For wound dressing materials, hydrogels are efficient in healing but cannot absorb large amount of blood and plasma. They are also not practical in terms of storage and transportation, needing special measures to prevent bacteria growth. Nanometer, micrometer, and macroscale drug delivery systems can extend half-life, optimize drug release rates, and reduce dosing frequency, making them suitable for personalized treatments of chronic wounds (Kim et al., 2019). Active ingredients released from carrier materials are also used in skincare repair or other cosmetic fields through transdermal delivery (Kim et al., 2020). Dry porous materials have good breathability and can absorb wound exudate. However, in case of large pores in freeze-dried gels problems may raise due to cells ingrowth which may cause wound breakdown and patient pain. Therefore, new dry porous materials combining high porosity and small pore dimensions should be developed. Such materials are aerogels.

Aerogels are dry, lightweight (density around 0.1–0.2 g/cm^3), nanostructured networks with high specific surface area (above 100 m^2/g) and open pores of few tens to few hundred nanometres (Aegerter, Leventis, Koebel, & Steiner, 2023). Classical aerogels are derived from inorganic (*e.g.* silica) or synthetic (*e.g.* resorcinol-formaldehyde) monomers; they are synthesised through sol-gel route and drying is usually performed with supercritical CO_2 ($scCO_2$) to avoid pores' collapse (Aegerter et al., 2023). A new generation of biomass-based aerogels was developed at the beginning of the 21st century, they are called bio-aerogels (Budtova et al., 2020; García-González et al., 2019; Thomas, Pothan, & Mavelil-Sam, 2018). Several polysaccharides have been used to make bio-aerogels: cellulose, marine polysaccharides (alginate, carrageenans), chitosan, pectin and starch (Budtova et al., 2020; Zhao et al., 2015). There is no literature reporting on neat CMC aerogels, *i.e.* materials with low density, high surface area and nanostructured morphology obtained *via* drying with $scCO_2$.

Because polysaccharides are already used in biomedical applications in the form of hydrogels, non-wovens and films, bio-aerogels have a huge potential as carriers for drug delivery, tissue engineering, wound dressing and biosensing (Nita, Ghilan, Rusu, Neamtu, & Chiriac, 2020). Bio-aerogels release drugs in a controlled way and can be simultaneously used as exudate absorbent (Bernardes et al., 2021). Compared to hydrogels, the advantages of aerogels are their high wound exudate absorption capacity, slow drug release, easy storage (as they are dry) and transportation (due to lightweight) (Groult, Buwalda, & Budtova, 2021a; Yahya et al., 2020).

To make a bio-aerogel, a polysaccharide should be first dissolved (here we do not consider nanocellulose or nanochitin suspensions). The next step is to make a 3D network which can be done by gelling the polymer solution or performing non-solvent induced phase separation (Budtova, 2019). If willing to preserve porous structure during drying, capillary forces should be avoided as they may lead to pores collapse. Drying with $scCO_2$ allows keeping open porosity resulting in material with meso- and small macropores (Aegerter et al., 2023).

Several studies have highlighted the potential of bio-aerogels as drug carriers (Barclay et al., 2019; Esquivel-Castro, Ibarra-Alonso, Oliva, & Martínez-Luévanos, 2019; García-González et al., 2021; Groult, Buwalda, & Budtova, 2022). In many cases drug is loaded from $scCO_2$ which is the technique limited to hydrophobic drugs (Falahati & Ghoreishi, 2019; García-González et al., 2021; Smirnova, Suttiruengwong, Seiler, & Arlt, 2005; Villegas, Oliveira, Bazito, & Vidinha, 2019). Another option is to impregnate a gel before drying, for example, in alcohol-based drug solution. Cellulose-pectin alcogels were impregnated with a theophylline dissolved in ethanol and dried with $scCO_2$ (Groult et al., 2022). Bacterial cellulose alcogels were immersed in ethanol solutions of dexpanthenol or L-ascorbic acid to obtain drug-loaded aerogels (Haimer et al., 2010). Impregnating the drug in a precursor before drying is simple but slow as it is a diffusion driven process. Finally, drug can be dissolved together with the polymer in the same solvent, followed by aerogel preparation route (Veronovski, Novak, & Knez, 2012). The main requirement here is that the drug should not be soluble in all subsequent fluids to avoid drug loss (García-González et al., 2021).

The goal of this work is to demonstrate the feasibility of making aerogels based on CMC using drying with supercritical CO_2; our hypothesis is that they can be used as carriers for drug release with properties different from those of known freeze-dried materials. As CMC aerogels have never been reported in literature, first we investigate the influence of CMC characteristics (molecular weight and DS) and of processing conditions (polymer concentration, type of non-solvent, presence of Ca^{2+} ions) on aerogels' density, specific surface area and morphology. Next, we used L-ascorbic acid 2-phosphate (Asc-2P) as a model drug to be released from CMC aerogels. Asc-2P is a stable phosphorylated derivative of ascorbic acid; it has been shown to have potential antioxidant capacity, angiogenesis-inducing capacity and ability to promote collagen synthesis by fibroblasts (Stumpf et al., 2011; Yu et al., 2018). This implies that it may be beneficial in promoting recovery from chronic wounds. We also used freeze-drying to make CMC "cryogels" to compare with the properties and performance of aerogel counterparts.

2. Materials and methods

2.1. Materials

Four different CMC samples, one with DS 0.7 and three with DS 0.9 were kindly provided by IFF. Their molecular weight was determined using viscometry (see Section 2.2). Before making solutions, CMC was dried at 50 °C in vacuum for at least 2 h, all concentrations are given in dry weight. Calcium chloride ($CaCl_2$), absolute ethanol and acetone were purchased from Fisher Chemical. Asc-2P was purchased from Sigma. Water was distilled.

2.2. Methods

2.2.1. Viscometry

The intrinsic viscosity [η] of CMC samples was determined using a capillary Ubbelohde Dilution Viscometer Type I with capillary diameter 0.63 mm and an iVisc system from LAUDA. The solvent was aqueous 0.01 M NaCl at 25.0 °C (Kulicke et al., 1996). The molecular weight (M_η) was calculated according to Mark-Houwink equation:

$$[\eta] = KM_\eta^{\alpha} \quad (1)$$

where $K = 1.43 \times 10^{-2}$ and $\alpha = 0.90$ as reported in Kulicke et al. (1996).

2.2.2. Preparation of CMC aerogels and cryogels

Aqueous CMC solutions of 1, 3 and 5 % wt/wt were prepared by mixing CMC powder and deionized water at room temperature. High viscosity solutions were placed in the centrifuge (Hettich® Universal 320/320R centrifuge) at 6000 rpm for 5 min to remove air bubbles. The resulting CMC solutions, transparent and optically homogeneous, were poured into cylindrical polypropylene vials with a diameter of 27.5 mm and left to rest for 48 h at room temperature. In some cases, $CaCl_2$ was added to CMC solution. The molar ratio (R) of metal cation (Me, mol/L)

to CMC carboxymethyl group ($RCOO^-$, mol/L) was calculated according to Eq. 2:

$$R = \frac{[Me]}{[RCOO^-]} \quad (2)$$

Solutions with R = 0.002, 0.004, 0.006 and 0.1 were prepared for comparison with the un-crosslinked CMC samples.

The pathways showing CMC aerogels and cryogels preparation are presented in Fig. 1. In order to perform $scCO_2$ drying to obtain aerogels, water in the CMC and CMC/$CaCl_2$ samples must be replaced by a fluid that is miscible with CO_2. Ethanol or acetone was slowly added on the top of the samples (volume 3–4 times exceeding CMC volume) leading to CMC coagulation. These samples were then washed in the corresponding non-solvent 6 times to completely remove water. As it will be shown in Results section, acetone was not suitable for making aerogels, and thus samples before $scCO_2$ drying were named "alcogels" (Fig. 1).

When using ethanol for solvent/non-solvent exchange, CMC solubility in ethanol/water should be considered in order not to "lose" the polymer during this processing step. The preliminary tests showed that CMC is soluble in ethanol/water mixtures when the concentration of ethanol is below 60–65 %. Thus, the concentration of ethanol during solvent/non-solvent exchanges was always kept above 70 %.

Drying with $scCO_2$ was performed at the centre PERSEE of Mines Paris-PSL as described elsewhere (Groult, Buwalda, & Budtova, 2021b; Zou & Budtova, 2021). First, the aerogel precursor was placed in a 1 L autoclave, and ethanol or acetone was added to cover the sample. The autoclave was closed, and dynamic washing with CO_2 at 50 bar and 37 °C was performed to wash out acetone or ethanol from the pores of the sample. The pressure was then increased to 80 bar, above CO_2 critical point. The system was maintained at 80 bar and 37 °C for 1–2 h to allow the $scCO_2$ to diffuse in the pores. A dynamic exchange of $scCO_2$ was then performed for 2 h. The system was slowly depressurized overnight to ambient conditions and aerogels collected. They were kept in a desiccator to prevent moisture absorption from the air.

To make cryogels, aqueous CMC was frozen in liquid nitrogen (−196 °C) for about 5 min, placed in the freeze-dryer (Cryotec Cosmos 80) and lyophilised at 40 mTorr (Fig. 1).

2.2.3. Shrinkage, density and porosity of CMC materials

The volume shrinkage of samples during the preparation steps was determined according to Eq. 3:

$$\text{Volume shrinkage } (\%) = \frac{V_0 - V_i}{V_0} \times 100\% \quad (3)$$

where V_0 represents the volume of the CMC solution before solvent exchange, and V_i represents the volume of the sample at the corresponding step, either after solvent exchange, or after drying.

The bulk density (ρ_{bulk}) was calculated as the ratio of sample mass (m) to the volume of dry matter (V):

$$\rho_{bulk} = \frac{m}{V} \quad (4)$$

The mass of the CMC samples was measured with digital analytical balance with a precision of 0.01 mg. The volume was measured with GeoPyc 1360 (Micromeritics) using the chamber of 19.1 mm diameter and applied force 21 N. Each sample was measured five times, and the error was <0.01 g/cm^3.

The porosity was estimated from bulk and skeletal densities:

$$\text{Porosity } (\%) = \left(1 - \frac{\rho_{bulk}}{\rho_{skeletal}}\right) \times 100\% \quad (5)$$

where $\rho_{skeletal}$ = 1.5 g/cm^3.

2.2.4. Specific surface area measurement (BET method)

The specific surface area was measured using nitrogen adsorption with the ASAP 2020 (Micromeritics) and Brunauer-Emmett-Teller (BET) method. The samples were degassed under vacuum at 70 °C for 10 h.

2.2.5. Scanning electron microscopy (SEM)

The internal morphology of the aerogels and cryogels was analysed with the SEM MAIA 3 (Tescan), equipped with a secondary and back-scattered electron detector. 14 nm of platinum was sputtered on sample surface with Q150T Quarum metallizer to prevent electrostatic charge build-up and image default. The observations were performed under accelerating voltage 3 kV.

2.2.6. Loading of Asc-2P

The preparation of Asc-2p loaded CMC aerogels and cryogels is schematically illustrated in Fig. 2. The Asc-2P (1 g/L) powder was added to CMC solution under stirring at room temperature. Drug-loaded aerogels and cryogels were obtained using $scCO_2$ and freeze-drying, respectively (Fig. 2).

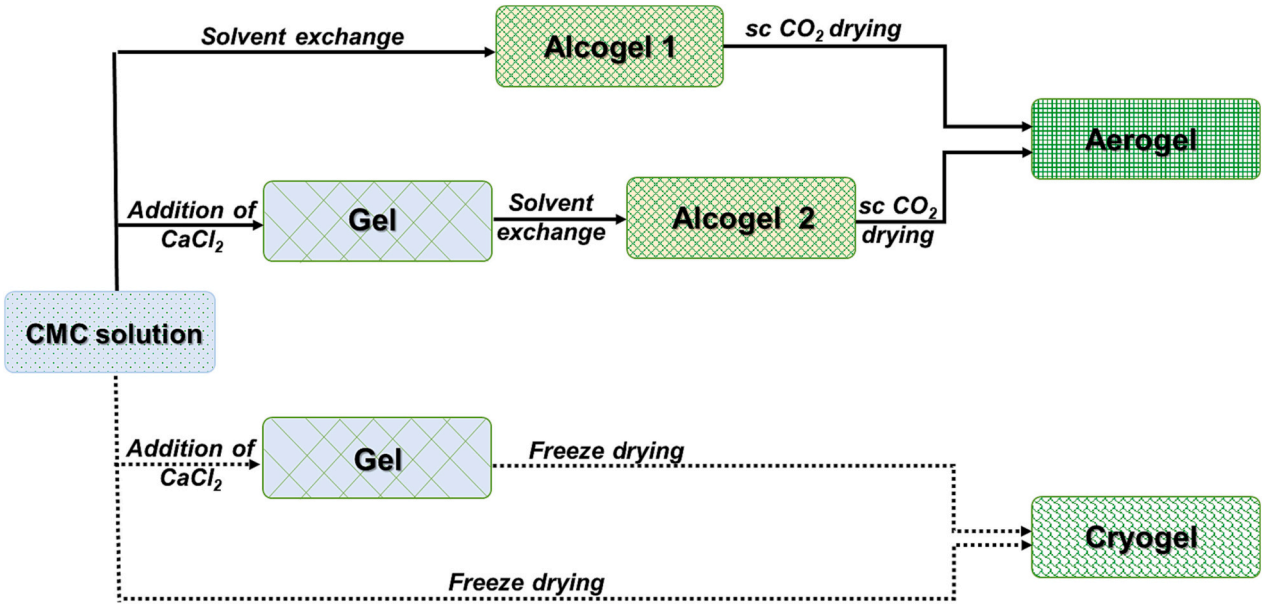

Fig. 1. Schematic presentation of CMC-based aerogels' and cryogels' preparation pathways.

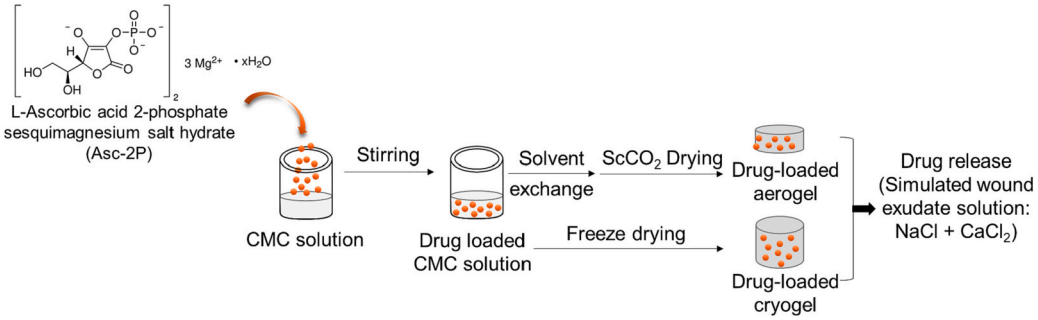

Fig. 2. Schematic illustration of the preparation of Asc-2P loaded CMC aerogels and cryogels.

2.2.7. Absorption of water and of SWE by aerogels and cryogels

The absorption and dissolution kinetics of aerogels and cryogels in distilled water and in SWE (8.298 g/L NaCl, 0.368 g/L $CaCl_2$, pH = 5.5; 37 °C, Slovenski Standard, 2002) was investigated by monitoring the swelling ratio:

$$\text{Swelling ratio } (\%) = \frac{Q(t)}{Q_0} \times 100\% \quad (6)$$

where Q(t) refers to sample weight at time t and Q_0 refers to the initial weight.

2.2.8. Asc-2P release experiments

The kinetics of drug release was investigated in sink conditions by immersing CMC aerogels or cryogels loaded with Asc-2P in SWE at 37 °C (the ratio sample weight/SWE volume was 0.001–0.002 g/mL). Drug concentration in the release bath was measured at 259 nm using a Peristaltic Sipper Pump 206-23790-91 and a 160C Sipper Unit coupled with Spectrophotometer UV-1800, all from Shimadzu. The measuring cell was with an optical path of 10 mm. The calibration dependence of absorbance as a function of drug concentration is given in Fig. S1 of the Supporting Information.

The drug loading efficiency and capacity of aerogels and cryogels of Asc-2P was calculated as follows:

$$\text{Drug loading efficiency } (\%) = \frac{M}{M_{max}} \times 100\% \quad (7)$$

where M refers to the amount of Asc-2P released at $t = \infty$ and M_{max} is the initial dose of drug in the solution.

$$\text{Loading capacity } (\%) = \frac{\text{drug dose in the sample (g)}}{\text{aerogel or cryogel weight (g)}} \times 100\% \quad (8)$$

The evolution of the cumulative release in time was calculated as follows:

$$\text{Cumulative release } (\%) = \frac{M(t)}{M} \times 100\% \quad (9)$$

where M(t) refers to the amount of Asc-2P in the release bath measured at time t, and M is the amount of Asc-2P released at $t = \infty$.

3. Results and discussion

3.1. Determination of CMC molecular weight

Four CMC samples were used in this work; their characteristics are presented in Table 1. The molecular weight was determined using viscometry, see details in Section 2.2.1. The dependence of the reduced viscosity on concentration for four CMC samples is shown in Fig. S2 of the Supporting Information. The values of the intrinsic viscosity together with the corresponding values of the molecular weight (see Eq. 1 in Section 2.2) are presented in Table 1. In the following, the samples will be named MxDy where x is CMC molecular weight and y corresponds to the DS.

Table 1
Degree of substitution, intrinsic viscosity, molecular weight, and samples' nomenclature.

DS	Intrinsic viscosity (mL/g)	M_η ($\times 10^4$ g·mol^{-1})	Nomenclature
0.9	460.37 ± 2.54	10 ± 0.05	M10D9
0.9	706.67 ± 8.01	16 ± 0.04	M16D9
0.9	1126.1 ± 13.05	28 ± 0.05	M28D9
0.7	741.16 ± 3.03	17 ± 0.05	M17D7

3.2. Visual observations, shrinkage, density and porosity of CMC aerogels and cryogels

The influence of non-solvent type ("aerogel" pathway), acetone and ethanol, on dry material properties was first studied. The photos of samples are presented in Fig. 3; freeze-dried materials are also shown for comparison. The samples obtained with acetone were strongly deformed (Fig. 3a), and a very high shrinkage occurred. The reason of such high

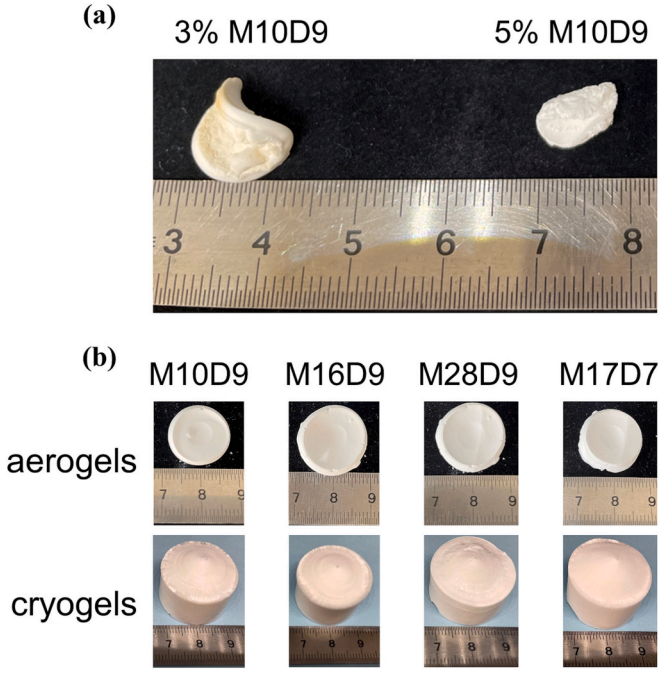

Fig. 3. The images of samples prepared with (a) acetone as non-solvent and dried with $scCO_2$ and (b) ethanol as non-solvent and dried with $scCO_2$ resulting in aerogels, all made from 5 % CMC solutions of different molecular weights. The corresponding cryogels made from the same starting solutions are also shown for comparison.

shrinkage is due to low affinity of CMC to acetone because of a strong difference in polarity; a similar result was obtained for hyaluronic acid coagulated in acetone (Aguilera-Bulla, Legay, Buwalda, & Budtova, 2022). Solubility parameters could help in quantifying this phenomenon, but neither Hansen or solubility parameters of CMC are not known except the value calculated using COMPASS Force Field, 24.35 $MPa^{1/2}$ (Derecskei & Derecskei-Kovacs, 2006), and the degree of substitution was not considered. The solubility parameters of ethanol and acetone are 26.5 $MPa^{1/2}$ and 19.9 $MPa^{1/2}$, respectively (Hansen, 2007). In the first approximation, it can be concluded that the solubility parameter of CMC is closer to that of ethanol compared to acetone, explaining CMC high shrinkage in acetone. The density of these samples was around 0.80–0.90 g/cm^3, indicating that acetone as non-solvent did not lead to the formation of aerogels. This pathway was thus not considered in the following, and only ethanol was used as a non-solvent. The examples of the aerogels obtained using ethanol are shown in Fig. 3b.

Total volume shrinkage (see Eq. 3 in Section 2.2.3) during the preparation of aerogels, from solution to aerogel, is high, around 80–90 %. Similar phenomenon has been reported for other bio-aerogels (Buchtová & Budtova, 2016; Zou & Budtova, 2021). An example of shrinkage during each processing step is shown in Fig. 4 for M17D7. Solvent/non-solvent exchange induced 70–80 vol.% shrinkage, and it is higher for lower polymer concentration in solution (Fig. 4 and Fig. S3 in the Supporting Information for all samples). Collapse of a swollen polymer coil in a non-solvent is well known for synthetic flexible polymers. CMC, being a semi-rigid polysaccharide, contracts in a non-solvent but not totally collapses, forming a 3D network (above the overlap concentration) with non-solvent in the pores. Such behavior has been reported for other polysaccharides during the preparation of bio-aerogels (Alnaief, Alzaitoun, García-González, & Smirnova, 2011; Budtova, 2019; Groult et al., 2021b). Freeze-drying resulted in the lower volume shrinkage (around 15–30 vol.%) compared to the total shrinkage for aerogels (see Fig. S3 in the Supporting Information for all samples).

Fig. 5a shows the influence of CMC concentration in the initial solution on bulk density of aerogels and cryogels for all CMC samples. The lower the concentration, the lower the density, as expected, and observed for other bio-aerogels (Gurikov, Raman, Griffin, Steiner, & Smirnova, 2019; Mandal, Donthula, Rewatkar, Sotiriou-Leventis, & Leventis, 2019; Sivaraman et al., 2022; Zou & Budtova, 2021). The cryogels have the lowest density, 0.01–0.07 g/cm^3; the density of CMC aerogels is between 0.04 and 0.25 g/cm^3. These values are similar to the bulk densities of cellulose aerogels previously reported in the literature for similar polymer concentration in the initial solution (Buchtová & Budtova, 2016; Buchtová, Pradille, Bouvard, & Budtova, 2019). The effect of molecular weight on aerogels' and cryogels' density is not significant within the studied range. All experimental data fall above density values calculated for a hypothetical case of zero shrinkage (dashed line in Fig. 5a).

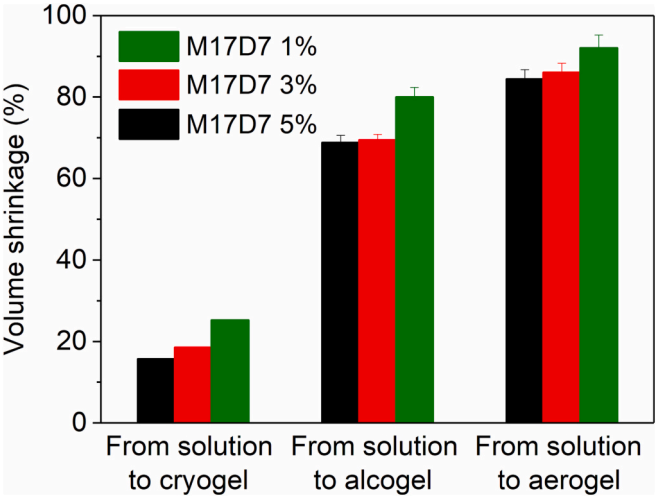

Fig. 4. Volume shrinkage during the preparation of M17D7 aerogels and cryogels from 1 %, 3 % and 5 % solutions.

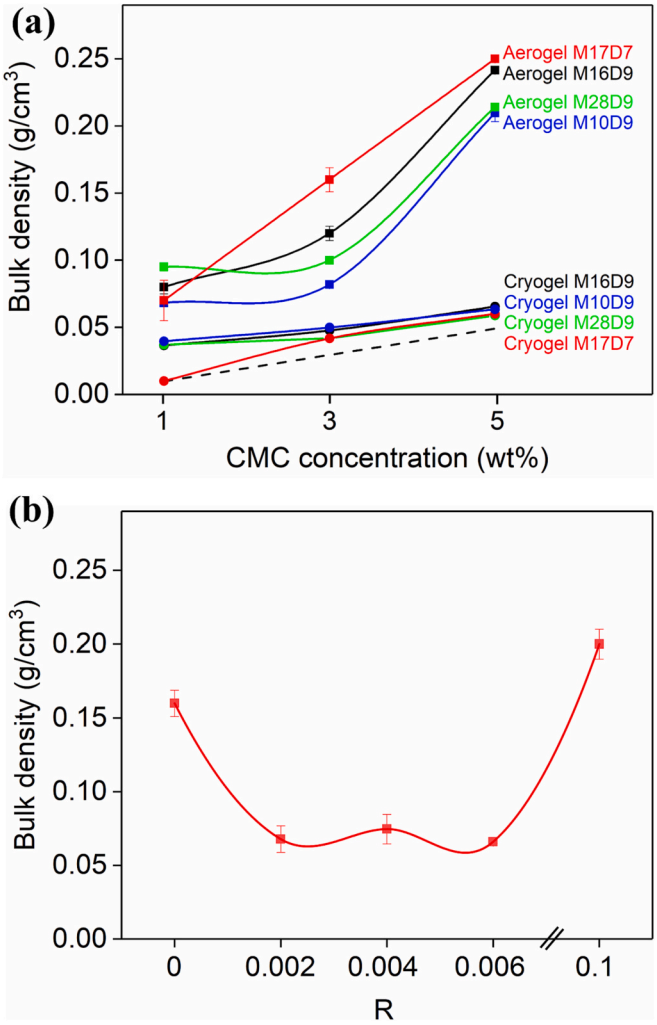

Fig. 5. Bulk density (a) of different CMC aerogels and cryogels as a function of CMC concentration in solution; dashed line is theoretical density corresponding to a case of zero volume shrinkage, and (b) of aerogels based on M17D7 made from 3 % solution as a function of the crosslinking ratio R. If the errors are not seen, they are smaller that symbols.

As all CMC samples demonstrated similar trends in shrinkage and density, one (M17D7) was selected to observe the effect of crosslinking with Ca^{2+} on aerogel density (Fig. 5b). The dependence on R has a U-shape curve; the reason is probably heterogeneous crosslinking resulting in inhomogeneous density distribution over sample volume.

The porosity of all aerogels and cryogels is above 80 % (Table S1), and it decreases with polymer concentration in solution, as expected. This result is similar to that reported in the literature, where the porosity of neat cellulose aerogels ranged from 86 % to 92 % and of cryogels around 97 % (Buchtová & Budtova, 2016). The porosity of calcium-crosslinked aerogels varies from 87 to 96 %.

3.3. Specific surface area and morphology of CMC aerogels and cryogels

Fig. 6a presents CMC aerogels' and cryogels' specific surface area as a function of CMC concentration in solution. Overall, aerogels have higher specific surface areas compared to cryogels, 30–143 m^2/g *vs* 5–18 m^2/g,

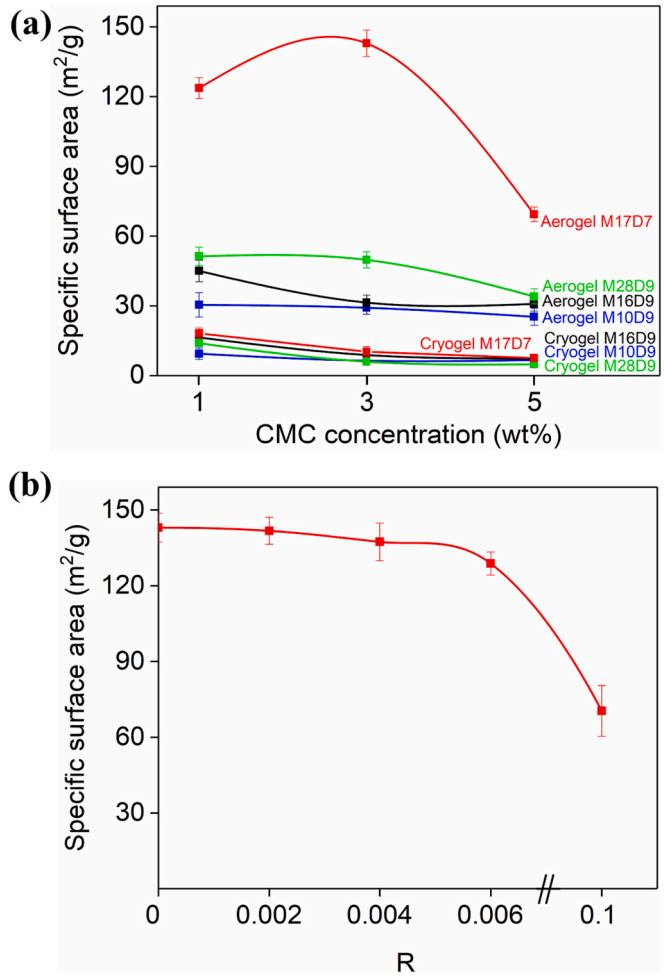

Fig. 6. Specific surface area (a) of CMC aerogels and cryogels as a function of CMC concentration in solution, and (b) of aerogels based on M17D7 (concentration in solution 3 %) as a function of the crosslinking ratio R.

respectively; a similar trend has been reported in literature for cellulose aerogels and cryogels (Buchtová et al., 2019; Buchtová & Budtova, 2016). Surprisingly, CMC and CMC/carbon nanotubes freeze-dried from water were reported with rather high specific surface area, around 110 m^2/g (Long et al., 2019). Aerogels based on CMC of the DS 0.9 possess rather low surface area, around 25–51 m^2/g *vs* 70–143 m^2/g for aerogels based on CMC of DS 0.7 (M17D7). Crosslinking with calcium of M17D7 aerogels made from 3 % solution induced the decrease of surface area with the increase of calcium concentration (Fig. 6b). It may be possible that crosslinking leads to the formation of dense non-porous polymer regions.

The morphology of aerogels based on M17D7 and M16D9 is shown on Fig. 7 together with the example of a M17D7 cryogel made from 3 % solution. The inner texture of the CMC materials strongly depends on the drying method. Aerogels, prepared by $scCO_2$ drying, present fine nanostructured fibrillated morphology (Fig. 7a, c, d). The M16D9 aerogel from 3 % solution has larger pores (around 230 nm as mean arithmetic value roughly estimated from SEM images, see pore size distribution in Fig. S4) compared to the 3 % M17D7 aerogel (around 150 nm), in correlation with lower specific surface area of the former (see Fig. 6a and 7d). Freeze-drying results in the network with sheet-like pore walls and large interconnected pores with diameter of several microns (mean arithmetic value 8 μm, see Fig. 7b and S4); such morphology is due to ice crystals growth during water freezing. The obtained morphology is similar to that of cryogels made from waxy maize starch solution (Zou & Budtova, 2021), which is not gelled before freezing as retrogradation of waxy maize starch solutions is very slow, of several weeks. The morphology of aerogels and cryogels correlate with specific surface area results: cryogels with very large macropores inherently possess a low specific surface area.

3.4. *Swelling and dissolution of CMC aerogels in water and in SWE*

To understand the kinetics of drug release from CMC aerogels and cryogels, the transformations of the porous material itself in contact with aqueous media was first analysed. Fig. 8 demonstrates the swelling ratio (Eq. 6) in water of aerogels and cryogels based on CMC of a similar molecular weight but of different DS, M16D9 and M17D7; density is also shown as it may influence swelling and dissolution. All materials first swell in water and then dissolve, thus showing dependences with maximum.

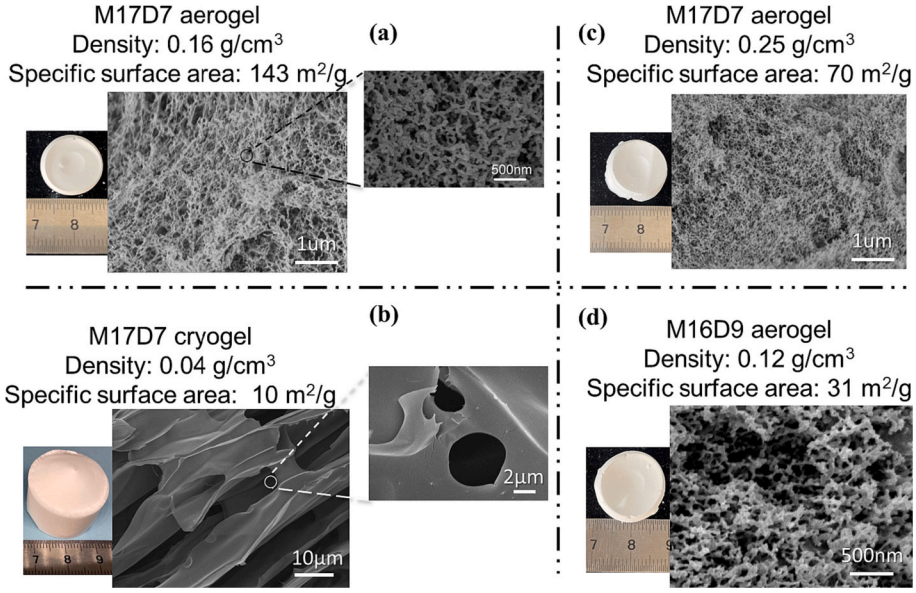

Fig. 7. SEM images of the cross-section of (a), (b) M17D7 aerogel and cryogel from 3 % solution, respectively and (c), (d) aerogels based on M17D7 from 5 % solution and M16D9 from 3 % solution, respectively.

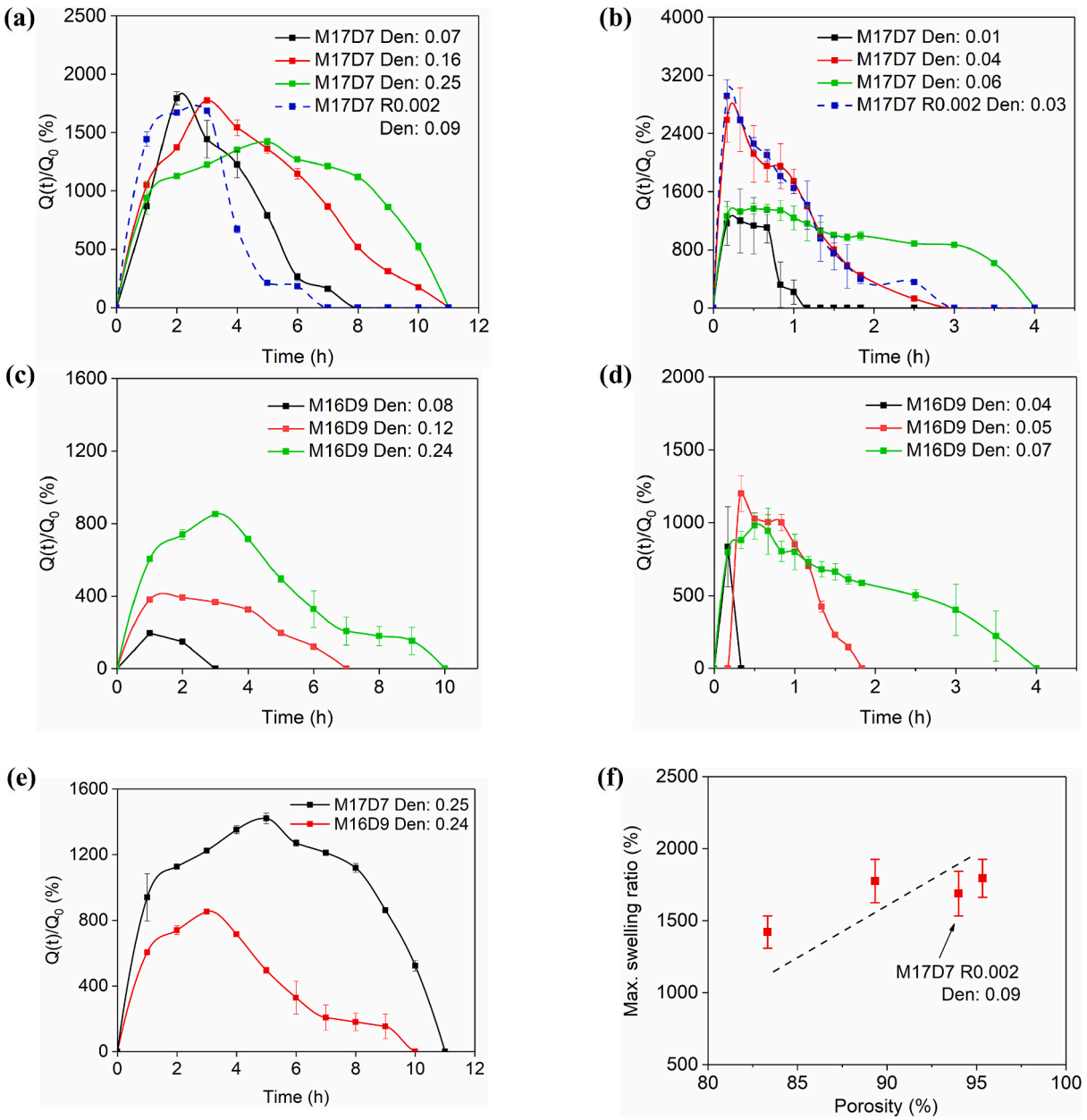

Fig. 8. Swelling ratio in water as a function of time of (a) M17D7 aerogels, (b) M17D7 cryogels, (c) M16D9 aerogels, (d) M16D9 cryogels, (e) comparison between aerogels M17D7 and M16D9 of a similar density (0.24–0.25 g/cm^3), (f) maximum swelling ratio of M17D7 aerogels as a function of porosity with the dashed line representing the linear trend.

Swelling and dissolution depend on polymer solubility, material density (or porosity) and morphology. In general, higher is porosity, higher is swelling (Ciuffarin et al., 2023), and thus, for the CMC of the same molecular weight and DS, cryogels swell more than aerogels (compare Fig. 8a and b, c and d, for aerogels and cryogels, respectively). This can also be seen in Fig. 8a for M17D7 aerogels of different densities; their maximum swelling as a function of porosity is summarised in Fig. 8f. The maximum value of swelling ratio of M17D7 aerogels is about 1900 % and of cryogels 2900 %.

The difference in the dissolution rate of aerogels and cryogels based on the same polymer mainly arises from material different density (or porosity) and morphology. Cryogels possess lower density compared to aerogels, leading to a faster dissolution of the former: for example, M17D7 cryogels of densities 0.01–0.04 g/cm^3 exhibit a faster dissolution compared to M17D7 aerogels of higher densities 0.16–0.25 g/cm^3 (Fig. 8a, b). For cryogels, water infiltration is fast due to large pores, and polymer concentration is low, both features leading to a faster dissolution compared to aerogels. The same trend, *i.e.* faster dissolution of cryogels compared to aerogels, was recorded for M16D9 (Fig. 8c, d).

Polymer solubility plays an important role in swelling and dissolution. Solubility is influenced by the DS; CMC with lower DS is less soluble in water than with the higher one (Kaewprachu, Jaisan, Rawdkuen, Tongdeesoontorn, & Klunklin, 2022). Fig. 8e shows swelling and dissolution of aerogels of similar density based on CMC of DS 0.7 and 0.9: because M16D9 is more soluble in water, it dissolves faster and thus swells less. In several cases the dissolution is so fast, that it results in low swelling. For example, M16D9 is highly soluble in water and aerogels of lower density (*i.e.* higher porosity) instead of high swelling possess low maximal swelling because of fast dissolution.

Crosslinking with calcium does not influence CMC aerogels swelling and dissolution for the case studied: M17D7 aerogels of the similar density (0.09 g/cm^3 and 0.07 g/cm^3), one crosslinked and the other not,

have very similar swelling and dissolution trend. This is most probably due to very low calcium concentration. Combining with the results on density, porosity and specific surface area, no advantage of using CMC crosslinked with Ca^{2+} was recorded, and these samples will not be used in the following.

As drug release was studied in the SWE, swelling and dissolution in this medium was also investigated. Fig. 9a and b shows the comparison of swelling and dissolution in water and in SWE for M16D9 and M17D7 aerogels. Interestingly, higher absorption was recorded in SWE, most probably because the dissolution was slower, see Table 2. The dissolution in SWE is slowed down because of the presence of salts. As in water, CMC of higher DS dissolves faster and swells less than its counterpart of lower DS (Table 2).

The comparison of swelling and dissolution of M17D7 aerogels of different density is presented in Fig. 9c, M17D7 cryogel is shown for comparison. As in water, lower density results in higher swelling. For example, M17D7 aerogel of density of 0.16 g/cm^3 possesses the highest capacity to absorb the SWE liquid (3000 %) compared to M17D7 of density 0.25 g/cm^3 (2500 %). As expected, M17D7 cryogel with density of 0.04 g/cm^3 shows highest capacity to absorption the SWE liquid (3913 %) and very fast dissolution. The direct proportionality between maximum swelling and porosity is demonstrated in Fig. 9d.

3.5. Asc-2P release from CMC aerogels and cryogels

Samples based on M17D7 (aerogels and cryogels) and on M16D9 (aerogels) were selected to load with Asc-2P and test drug release kinetics. First, density and specific surface area of drug-loaded CMC were measured. Overall, the characteristics of loaded materials are similar to those of their neat counterparts (Table S2); some decrease in specific surface area, within 10–20 %, may be explained by drug blocking small pores in CMC aerogels.

The loading efficiency (Eq. 7) of cryogels is 100 %, as expected, with no drug loss during freeze-drying. However, loading efficiency of aerogels is around 50–60 %. The reason is that Asc-2P could be partly washed-out during water to ethanol exchange; some washing out could have also occurred during supercritical drying due to CO_2 circulation. A similar phenomenon was reported for pectin aerogels loaded with theophylline (Groult et al., 2021b) and chitosan aerogels loaded with dexamethasone phosphate (Chartier et al., 2023). Still the values obtained are similar to the results reported in literature for other bio-aerogels, based on starch, alginate, cellulose, chitosan or pectin (Esquivel-Castro et al., 2019; Groult et al., 2022; Mehling, Smirnova, Guenther, & Neubert, 2009).

Table 2
Maximum swelling ratio and dissolution time of aerogels of a similar density based on CMC of the similar molecular weight.

	Max. swelling ratio (%)		Dissolution time (h)	
	In water	In SWE	In water	In SWE
M16D9 aerogel Density: 0.24 g/cm^3	853 ± 20	1426 ± 168	~10	~23
M17D7 aerogel Density: 0.25 g/cm^3	1421 ± 32	2454 ± 74	~11	~48

The Asc-2P loading capacity (Eq. 8) of the CMC aerogels and cryogels, ranging from 2 % to 3.38 %, is similar to the loading capacities observed for theophylline in cellulose-pectin composite aerogels (from 2 to 4 %) (Groult et al., 2022). However, it is markedly lower than the loading capacities reported for other drugs in various bio-aerogels, which range from 15 % to 80 % (Barclay et al., 2019; Esquivel-Castro et al., 2019; García-González et al., 2021; Groult et al., 2022; Mehling et al., 2009; Ulker & Erkey, 2014). It is important to note that the loading capacity strongly depends on the method of drug incorporation, its initial concentration and solubility.

The release of Asc-2P from CMC aerogels and cryogels was monitored in SWE (pH = 5.5, 37 °C) to simulate the physiological conditions of the wound environment. Fig. 10a and b shows the examples of the cumulative release M(t)/M (M the total mass of released drug) of Asc-2P from M16D9 and M17D7 aerogels and cryogel as a function of time t; samples' densities are also noted. The corresponding swelling and dissolution of each sample are shown by dashed lines. The photos of

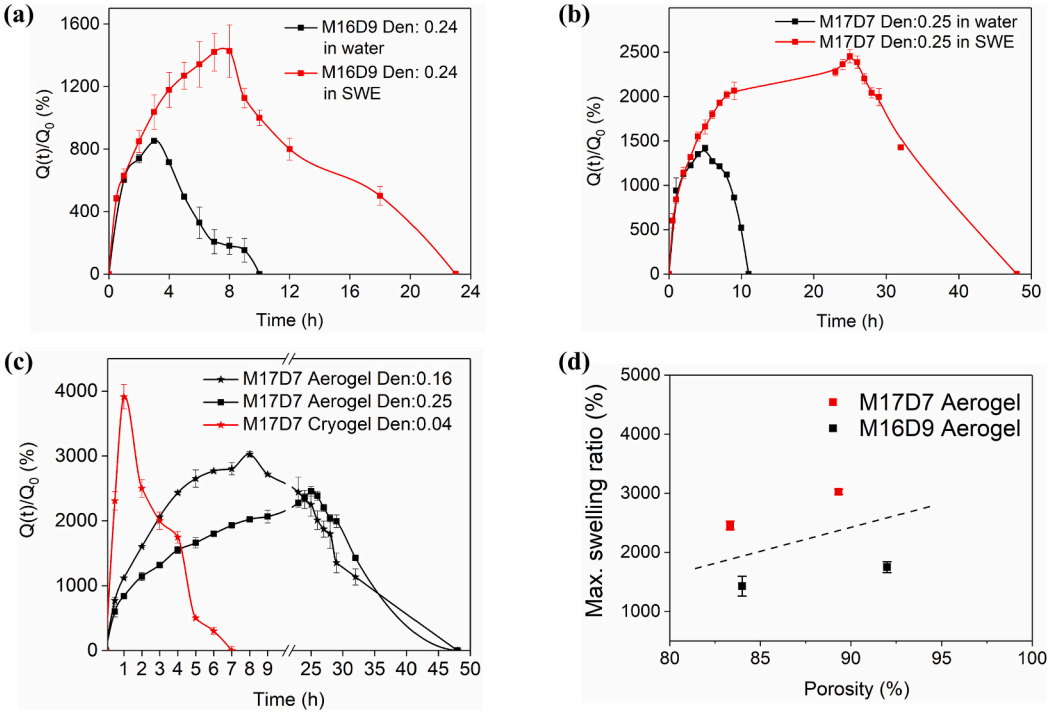

Fig. 9. Swelling ratio in water and in SWE as a function of time of (a) M16D9 aerogels, (b) M17D7 aerogel; (c) M17D7 aerogels of different density and M17D7 cryogel; (d) maximum swelling ratio in SWE of aerogels as a function of porosity with the dashed line representing the linear trend.

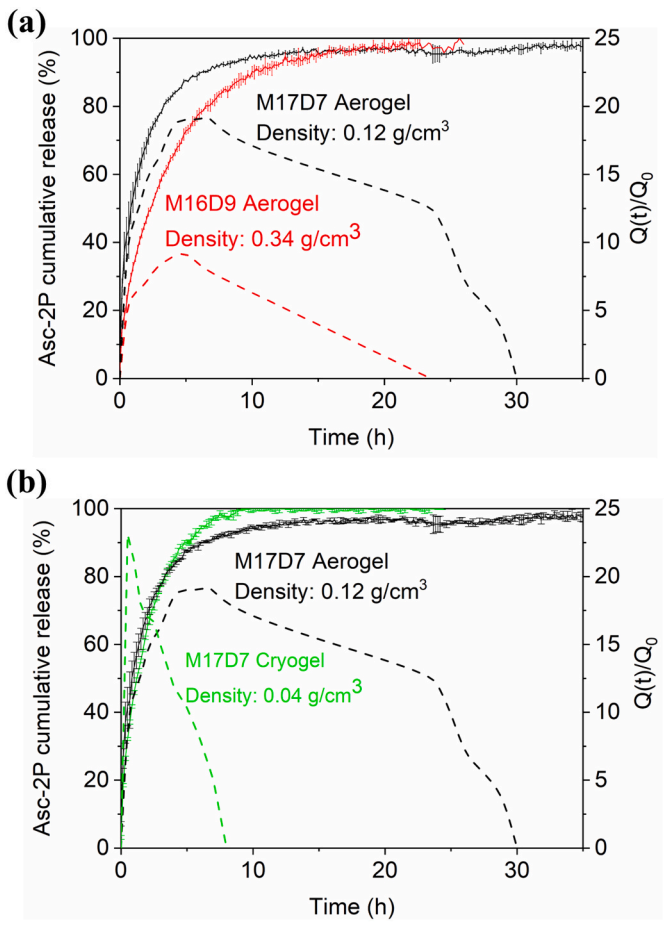

Fig. 10. Asc-2P cumulative release (%) over time from (a) M17D7 aerogel and M16D9 aerogel, and (b) from M17D7 aerogel and M17D7 cryogel.

samples at different stages of release are presented in Fig. S5.

Drug release kinetics can be divided into two steps which are closely related to CMC swelling and dissolution. During the first few hours of the immersion in SWE, all samples demonstrate a rapid increase in mass as a result of the absorption of the release medium (Fig. 10a–b), and drug release is fast. During this swelling step, drug release from M17D7 is faster than from M16D9 as M17D7 aerogel is of lower density; the same was reported for drug release from various bio-aerogels (Chartier et al., 2023; Groult et al., 2021b). In approximately 5 h, both M16D9 and M17D7 aerogels reach their maximum swelling which is lower for M16D9 because of higher density, as also demonstrated in Fig. 8. Having high affinity to water, M16D9 aerogel dissolves right after it reached the maximum swelling. Total dissolution occurs after 23–25 h, and Asc-2P release is terminated at the same moment. The competition between swelling and dissolution of the less hydrophilic M17D7 aerogel leads to a longer dissolution, about 30 h. However, because of the fast release at the first stage, all drug is released from M17D7 at practically the same time as from M16D9.

The comparison of the release from aerogel and cryogel, both based on M17D7, is shown in Fig. 10b. The swelling and dissolution of the cryogel was very fast, and so was Asc-2P release which was finished in 10 h, even before complete cryogel dissolution. This fast release is attributed to cryogel very low density and pores' large dimensions (see Fig. 7b).

To analyse the release kinetics, Fick approach was tested by plotting the Asc-2P cumulative release as a function of $\sqrt{t}$ (Fig. S6). Fick approach is widely used for the analysis of drug release kinetics, membrane formation due to phase separation and also for cellulose regeneration from cellulose-*N*-methylmorpholine-N-oxide monohydrate or from cellulose-NaOH-water solutions and gels (Gavillon & Budtova, 2007). For all cases studied M(t)/M *vs* $\sqrt{t}$ were straight lines up to 60–70 % of cumulative release (Fig. S6), allowing using Fick approach to calculate drug diffusion coefficient. This result, surprising from the first glance for eroding or dissolving drug carriers, is explained by the fact that 70–80 % of Asc-2P diffusion occurs during CMC swelling and not dissolution.

Classical diffusion approach for a semi-infinite plane was used to describe the release kinetics, and early-time and half-time approximations were used to calculate Asc-2P diffusion coefficients:

$$\frac{M(t)}{M} = 1 - \sum_{n=0}^{\infty} \frac{8}{(2n+1)^2\pi^2} exp\left(\frac{-D\pi^2 t(2n+1)^2}{l^2}\right) \quad (10)$$

where D is the diffusion coefficient, and l is sample half thickness.

Early-time approximation ($0 \le M(t)/M \le 0.6$):

$$\frac{M(t)}{M} = 4\sqrt{\frac{Dt}{\Pi l^2}} \quad (11)$$

Half-time approximation:

$$D = 0.049 \Big/ \sqrt{(t/l^2)} \quad (12)$$

where $\sqrt{(t/l^2)}$ is the abscissa when $M(t)/M = 0.5$.

The diffusion coefficients are presented in Table 3, and the corresponding fits to the experimental data using Eq. 10 are in Fig. 11. The calculated release with the diffusion coefficient determined from early-time approximation shows the best fit to experimental data. As expected, drug diffusion from M17D7 cryogel (density: 0.04 g/cm^3) is significantly faster than from the other two samples (Table 3). This rapid drug release is due to the highly macroporous open-pores morphology of the cryogel (Fig. 7b), which is a result of the growth of water ice crystals during freeze drying. This highly open structure facilitates rapid intake of the release medium, and then a fast drug diffusion throughout the system. The combination of fast solvent penetration and a low-density network likely contributes to accelerated carrier dissolution and, consequently, the rapid release of the drug.

The diffusion from the M17D7 aerogel (density: 0.12 g/cm^3) was twice faster than that from M16D9 aerogel (density: 0.34 g/cm^3) due to the lower density of the former, while the morphologies are visually similar (Fig. 7). Faster and higher swelling of M17D7 leads to faster drug release. The results obtained show that the drug release can be tuned *via* CMC density, morphology and degree of substitution. The diffusion coefficients of Asc-2P release from CMC aerogels and cryogels are of the same order of magnitude as those of drugs (cyclohexanone, acetaminophen, phenacetin and cafein) released from cellulose ether hydrogels (10^{-9}–10^{-10} m^2/s) (Caccavo, Cascone, Lamberti, & Barba, 2015; Favre & Girard, 2001; Ferrero, Massuelle, Jeannerat, & Doelker, 2008, 2013; Ferrero, Massuelle, & Doelker, 2010). This suggests that CMC aerogels and cryogels have potential applications in fields related to drug delivery and controlled release.

4. Conclusions

This work demonstrated the feasibility of making new materials,

Table 3
Diffusion coefficients of Asc-2P during release from aerogels and cryogel in SWE at 37 °C.

Samples	M17D7 aerogel	M17D7 cryogel	M16D9 aerogel
Density (g/cm^3)	0.12 ± 0.01	0.04	0.34 ± 0.02
D (×10^{-9} m^2/s)-early time	5.02 ± 0.46	21.37 ± 0.62	2.37 ± 0.24
D (×10^{-9} m^2/s)-half time	6.19 ± 0.58	21.80 ± 0.40	2.48 ± 0.11

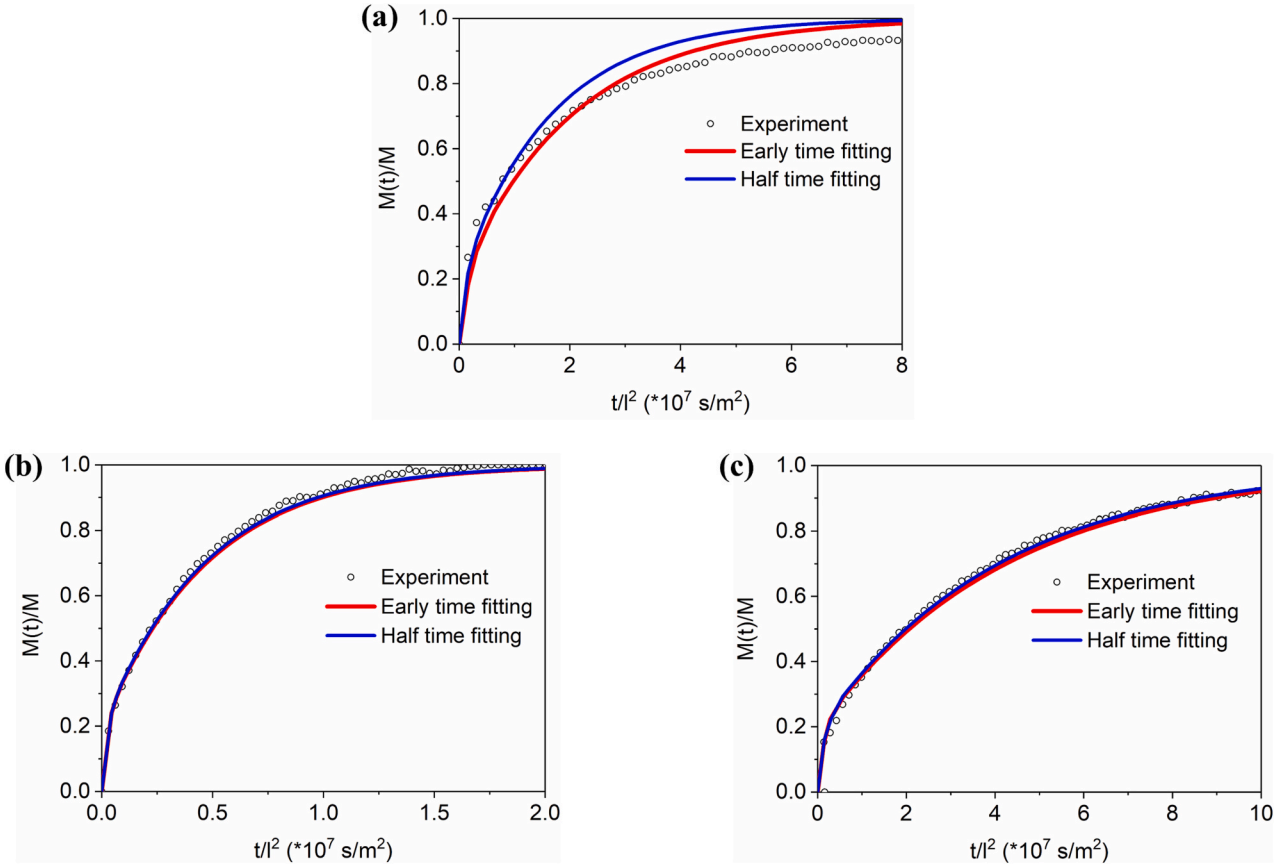

Fig. 11. Kinetics of the Asc-2P release in SWE of 37 °C from the (a) M17D7 aerogel (density: 0.12 g/cm^3), (b) M17D7 cryogel (density: 0.04 g/cm^3) and (c) M16D9 aerogel (density: 0.34 g/cm^3) samples.

neat CMC aerogels: they are with open pores, of low density and nanostructured, with high specific surface area up to 143 m^2/g. The preparation consisted of CMC dissolution in water followed by non-solvent induced phase separation in ethanol and drying with supercritical CO_2. Coagulation in acetone did not result in aerogels as material density was high. The molecular weight of CMC and the DS did not significantly impact aerogels density, but lower DS resulted in much higher specific surface area. The same CMC solutions were also freeze-dried, resulting in highly macroporous ultralight materials (density 0.01–0.07 g/cm^3) with low surface area, in the range of 5–18 m^2/g.

The internal morphology of aerogels and cryogels is quite different: aerogels possess net-like fine structure while cryogels are with sheet-like pore walls and large pores and channels of several microns. Drying with $scCO_2$ retained the nanostructured pores formed during CMC coagulation, whereas the growth of ice crystals during freezing resulted in dense pore walls and large macropores.

Aerogels' and cryogels' swelling and dissolution in water and in SWE was investigated in the view of testing these materials for drug delivery. Cryogels were swelling more and dissolving faster than their aerogel counterparts. Porosity, morphology and solubility were shown to influence porous CMC swelling and dissolution. For aerogels based on less water-soluble CMC (samples M17D7, *i.e.* with DS 0.7) higher porosity induced higher swelling while for M16D9 aerogels (*i.e.* DS 0.9) the opposite behavior was recorded. Aerogels of the same density but based on CMC M16D9 were dissolving faster and thus swelling less than M17D7 aerogels.

CMC aerogels and cryogels were tested as drug delivery devices. A very simple procedure was used for drug loading: Asc-2P was dissolved together with CMC, and drug-loaded CMC aerogels and cryogels were made using the same process as for neat materials. The loading efficiency of aerogels was around 50–70 % and of cryogels 100 %. The duration of complete release increased with material density: it was around 23–25 h for aerogels and twice lower for cryogels. The release kinetics of Asc-2P from aerogels and cryogels was shown to be governed by Fickian diffusion and controlled by material density and swelling/dissolution, with M17D7 cryogel (density = 0.04 g/cm^3) having the highest diffusion coefficient and M16D9 aerogel (density = 0.34 g/cm^3) the lowest.

In summary, we demonstrated that various CMC porous materials, aerogels and cryogels, can be prepared by varying the CMC concentration in solution and drying method. CMC aerogels and cryogels can potentially be used in the biomedical field as drug delivery matrices with tuneable properties. As this is the first report on CMC aerogels obtained *via* drying with supercritical CO_2, still a lot of work needs to be done for these materials to be used in practice (*in-vitro* and *in-vivo* bio-medical tests, exploring scalability and reducing production costs, life cycle assessment, etc). For applications that demand high drug loading and rapid release, cryogels might be the preferred choice. Conversely, if a sustained release over an extended period is required, aerogels would be a better option. We provided different "recipes" of making porous CMC materials with properties that can be adjusted to specific requirements of the application in cosmetics, personal care, pharmacology and medicine.

CRediT authorship contribution statement

Sujie Yu: Writing – review & editing, Writing – original draft, Methodology, Investigation, Formal analysis, Data curation. **Tatiana Budtova:** Writing – review & editing, Validation, Supervision, Resources, Project administration, Methodology, Investigation, Formal analysis, Conceptualization.

Declaration of competing interest

The authors declare no competing financial interest.

Data availability

Data will be made available on request.

Acknowledgements

We are grateful to China Scholarship Council for funding, to IFF for providing CMC samples, to J. Jaxel (PERSEE, Mines Paris) for supercritical drying and to I. Lahouij and F. Georgi (CEMEF, Mines Paris) for guiding in SEM analysis, and to C. Chartier, M. Négrier, L. Legay and L. Gelas for helpful advices.

Appendix A. Supplementary data

Supplementary data to this article can be found online at https://doi.org/10.1016/j.carbpol.2024.121925.

References

Aegerter, M. A., Leventis, N., Koebel, M. M., & Steiner, S. A. (2023). *Springer handbook of aerogels* (2nd ed., pp. 1–1800). Springer Nature Switzerland AG.

Aguilera-Bulla, D., Legay, L., Buwalda, S. J., & Budtova, T. (2022). Crosslinker-free hyaluronic acid aerogels. *Biomacromolecules, 23*(7), 2838–2845.

Alnaief, M., Alzaitoun, M. A., García-González, C. A., & Smirnova, I. (2011). Preparation of biodegradable nanoporous microspherical aerogel based on alginate. *Carbohydrate Polymers, 84*(3), 1011–1018.

Barclay, T. G., Day, C. M., Petrovsky, N., & Garg, S. (2019). Review of polysaccharide particle-based functional drug delivery. *Carbohydrate Polymers, 221*, 94–112.

Bernardes, B. G., Del Gaudio, P., Alves, P., Costa, R., García-Gonzaléz, C. A., & Oliveira, A. L. (2021). Bioaerogels: Promising nanostructured materials in fluid management, healing and regeneration of wounds. *Molecules, 26*(13), 3834.

Buchtová, N., & Budtova, T. (2016). Cellulose aero-, cryo- and xerogels: Towards understanding of morphology control. *Cellulose, 23*(4), 2585–2595.

Buchtová, N., Pradille, C., Bouvard, J. L., & Budtova, T. (2019). Mechanical properties of cellulose aerogels and cryogels. *Soft Matter, 15*, 7901–7908.

Budtova, T. (2019). Cellulose II aerogels: a review. *Cellulose, 26*(1), 81–121.

Budtova, T., Aguilera, D. A., Beluns, S., Berglund, L., Chartier, C., Espinosa, E., Gaidukovs, S., Klimek-Kopyra, A., Kmita, A., Lachowicz, D., Liebner, F., Platnieks, O., Rodríguez, A., Tinoco Navarro, L. K., Zou, F. X., & Buwalda, S. J. (2020). Biorefinery approach for aerogels. *Polymers, 12*(12), 2779.

Buhus, G., Peptu, C., Popa, M., & Desbrières, J. (2009). Controlled release of water soluble antibiotics by carboxymethylcellulose-and gelatin-based hydrogels crosslinked with epichlorohydrin. *Cellulose Chemistry and Technology, 43*(4), 141–151.

Caccavo, D., Cascone, S., Lamberti, G., & Barba, A. A. (2015). Modelling the drug release from hydrogel-based matrices. *Molecular Pharmaceutics, 12*(2), 474–483.

Chartier, C., Buwalda, S., Ilochonwu, B. C., Van Den Berghe, H., Bethry, A., Vermonden, T., … Budtova, T. (2023). Release kinetics of dexamethasone phosphate from porous chitosan: Comparison of aerogels and cryogels. *Biomacromolecules, 24*(10), 4494–4501.

Ciuffarin, F., Négrier, M., Plazzotta, S., Libralato, M., Calligaris, S., Budtova, T., & Manzocco, L. (2023). Interactions of cellulose cryogels and aerogels with water and oil: Structure-function relationships. *Food Hydrocolloids, 140*, Article 108631.

Derecskei, B., & Derecskei-Kovacs, A. (2006). Molecular dynamic studies of the compatibility of some cellulose derivatives with selected ionic liquids. *Molecular Simulation, 32*(2), 109–115.

Esquivel-Castro, T. A., Ibarra-Alonso, M. C., Oliva, J., & Martínez-Luévanos, A. (2019). Porous aerogel and core/shell nanoparticles for controlled drug delivery: A review. *Materials Science and Engineering: C, 96*, 915–940.

Falahati, M. T., & Ghoreishi, S. M. (2019). Preparation of balangu (*Lallemantia royleana*) seed mucilage aerogels loaded with paracetamol: Evaluation of drug loading *via* response surface methodology. *The Journal of Supercritical Fluids, 150*, 1–10.

Favre, E., & Girard, S. (2001). Release kinetics of low molecular weight solutes from mixed cellulose ethers hydrogels: A critical experimental study. *European Polymer Journal, 37*(8), 1527–1532.

Ferrero, C., Massuelle, D., & Doelker, E. (2010). Towards elucidation of the drug release mechanism from compressed hydrophilic matrices made of cellulose ethers. II. Evaluation of a possible swelling-controlled drug release mechanism using dimensionless analysis. *Journal of Controlled Release, 141*(2), 223–233.

Ferrero, C., Massuelle, D., Jeannerat, D., & Doelker, E. (2008). Towards elucidation of the drug release mechanism from compressed hydrophilic matrices made of cellulose ethers. I. Pulse-field-gradient spin-echo NMR study of sodium salicylate diffusivity in swollen hydrogels with respect to polymer matrix physical structure. *Journal of Controlled Release, 128*(1), 71–79.

Ferrero, C., Massuelle, D., Jeannerat, D., & Doelker, E. (2013). Towards elucidation of the drug release mechanism from compressed hydrophilic matrices made of cellulose ethers. III. Critical use of thermodynamic parameters of activation for modeling the water penetration and drug release processes. *Journal of Controlled Release, 170*(2), 175–182.

García-González, C. A., Budtova, T., Durães, L., Erkey, C., Del Gaudio, P., Gurikov, P., … Smirnova, I. (2019). An opinion paper on aerogels for biomedical and environmental applications. *Molecules, 24*(9), 1815.

García-González, C. A., Sosnik, A., Kalmár, J., De Marco, I., Erkey, C., Concheiro, A., & Alvarez-Lorenzo, C. (2021). Aerogels in drug delivery: From design to application. *Journal of Controlled Release, 332*, 40–63.

Gavillon, R., & Budtova, T. (2007). Kinetics of cellulose regeneration from cellulose−NaOH−water gels and comparison with cellulose−*N*-methylmorpholine–*N*-oxide−water solutions. *Biomacromolecules, 8*(2), 424–432.

Groult, S., Buwalda, S., & Budtova, T. (2021a). Pectin hydrogels, aerogels, cryogels and xerogels: Influence of drying on structural and release properties. *European Polymer Journal, 149*, Article 110386.

Groult, S., Buwalda, S., & Budtova, T. (2021b). Tuning bio-aerogel properties for controlling theophylline delivery. Part 1: Pectin aerogels. *Materials Science & Engineering C, 126*, Article 112148.

Groult, S., Buwalda, S., & Budtova, T. (2022). Tuning bio-aerogel properties for controlling drug delivery. Part 2: Cellulose-pectin composite aerogels. *Biomaterials Advances, 135*, Article 212732.

Gurikov, P., Raman, S. P., Griffin, J. S., Steiner, S. A., & Smirnova, I. (2019). 110th anniversary: Solvent exchange in the processing of biopolymer aerogels: Current status and open questions. *Industrial and Engineering Chemistry Research, 58*(40), 18590–18600.

Haimer, E., Wendland, M., Schlufter, K., Frankenfeld, K., Miethe, P., Potthast, A., … Liebner, F. (2010). Loading of bacterial cellulose aerogels with bioactive compounds by antisolvent precipitation with supercritical carbon dioxide. *Macromolecular Symposia, 294*(2), 64–74.

Hansen, C. M. (2007). *Hansen solubility parameters: A user's handbook* (2nd ed.). Boca Raton: CRC Press.

Kaewprachu, P., Jaisan, C., Rawdkuen, S., Tongdeesoontorn, W., & Klunklin, W. (2022). Carboxymethyl cellulose from young palmyra palm fruit husk: Synthesis, characterization, and film properties. *Food Hydrocolloids, 124*, Article 107277.

Kanafi, N. M., Rahman, N. A., & Rosdi, N. H. (2019). Citric acid cross-linking of highly porous carboxymethyl cellulose/poly(ethylene oxide) composite hydrogel films for controlled release applications. *Materials Today: Proceedings, 7*, 721–731.

Kanikireddy, V., Varaprasad, K., Jayaramudu, T., Karthikeyan, C., & Sadiku, R. (2020). Carboxymethyl cellulose-based materials for infection control and wound healing: A review. *International Journal of Biological Macromolecules, 164*, 963–975.

Kim, B., Cho, H. E., Moon, S. H., Ahn, H. J., Bae, S., Cho, H. D., & An, S. (2020). Transdermal delivery systems in cosmetics. *Biomedical Dermatology, 4*, 1–12.

Kim, H. S., Sun, X., Lee, J. H., Kim, H. W., Fu, X., & Leong, K. W. (2019). Advanced drug delivery systems and artificial skin grafts for skin wound healing. *Advanced Drug Delivery Reviews, 146*, 209–239.

Kulicke, W. M., Kull, A. H., Kull, W., Thielking, H., Engelhardt, J., & Pannek, J. B. (1996). Characterization of aqueous carboxymethylcellulose solutions in terms of their molecular structure and its influence on rheological behaviour. *Polymer, 37*(13), 2723–2731.

Lin, R., Li, A., Lu, L., & Cao, Y. (2015). Preparation of bulk sodium carboxymethyl cellulose aerogels with tunable morphology. *Carbohydrate Polymers, 118*, 126–132.

Liu, P., Zhai, M., Li, J., Peng, J., & Wu, J. (2002). Radiation preparation and swelling behavior of sodium carboxymethyl cellulose hydrogels. *Radiation Physics and Chemistry, 63*(3–6), 525–528.

Long, L., Li, F., Shu, M., Zhang, C., & Weng, Y. (2019). Fabrication and application of carboxymethyl cellulose-carbon nanotube aerogels. *Materials, 12*(11), 1867.

Mandal, C., Donthula, S., Rewatkar, P. M., Sotiriou-Leventis, C., & Leventis, N. (2019). Experimental deconvolution of depressurization from capillary shrinkage during drying of silica wet-gels with SCF CO_2 why aerogels shrink? *Journal of Sol-Gel Science and Technology, 92*(3), 662–680.

Mbituyimana, B., Liu, L., Ye, W., Ode Boni, B. O., Zhang, K., Chen, J., Thomas, S., Vasilievich, R. V., Shi, Z., & Yang, G. (2021). Bacterial cellulose-based composites for biomedical and cosmetic applications: Research progress and existing products. *Carbohydrate Polymers, 273*, Article 118565.

Mehling, T., Smirnova, I., Guenther, U., & Neubert, R. H. H. (2009). Polysaccharide-based aerogels as drug carriers. *Journal of Non-Crystalline Solids, 355*(50–51), 2472–2479.

Nayak, S., & Kundu, S. C. (2014). Sericin-carboxymethyl cellulose porous matrices as cellular wound dressing material: Sericin-carboxymethyl cellulose porous matrices. *Journal of Biomedical Materials Research Part A, 102*(6), 1928–1940.

Nita, L. E., Ghilan, A., Rusu, A. G., Neamtu, I., & Chiriac, A. P. (2020). New trends in bio-based aerogels. *Pharmaceutics, 12*(5), 449.

Rothe, H., Rost, J., Kramer, F., Alkhatib, Y., Petzold-Welcke, K., Klemm, D., Fischer, D., & Liefeith, K. (2022). Bacterial nanocellulose: Reinforcement of compressive strength using an adapted Mobile Matrix Reservoir Technology and suitable post-modification strategies. *Journal of the Mechanical Behavior of Biomedical Materials, 125*, Article 104978.

Sadeghi, S., Nourmohammadi, J., Ghaee, A., & Soleimani, N. (2020). Carboxymethyl cellulose-human hair keratin hydrogel with controlled clindamycin release as antibacterial wound dressing. *International Journal of Biological Macromolecules, 147*, 1239–1247.

Seddiqi, H., Oliaei, E., Honarkar, H., Jin, J., Geonzon, L. C., Bacabac, R. G., & Klein-Nulend, J. (2021). Cellulose and its derivatives: Towards biomedical applications. *Cellulose, 28*(4), 1893–1931.

Sivaraman, D., Siqueira, G., Maurya, A. K., Zhao, S., Koebel, M. M., Nyström, G., Lattuada, M., & Malfait, W. J. (2022). Superinsulating nanocellulose aerogels: Effect of density and nanofiber alignment. *Carbohydrate Polymers, 292*, Article 119675.

Slovenski Standard, EN 13726-1:2002 (2002). Test methods for primary wound dressings — Part 1: Aspects of absorbency, Section 3.6, dispersion characteristics.

Smirnova, I., Suttiruengwong, S., Seiler, M., & Arlt, W. (2005). Dissolution rate enhancement by adsorption of poorly soluble drugs on hydrophilic silica aerogels. *Pharmaceutical Development and Technology, 9*(4), 443–452.

Stumpf, U., Michaelis, M., Klassert, D., Cinatl, J., Altrichter, J., Windolf, J., Hergenröther, J., & Scholz, M. (2011). Selection of proangiogenic ascorbate derivatives and their exploitation in a novel drug-releasing system for wound healing. *Wound Repair and Regeneration, 19*(5), 597–607.

Thomas, S., Pothan, L. A., & Mavelil-Sam, R. (2018). *Biobased aerogels: Polysaccharide and protein-based materials* (1st ed.) (1st ed., Vol. 58). UK: Royal Society of Chemistry.

Ulker, Z., & Erkey, C. (2014). An emerging platform for drug delivery: Aerogel based systems. *Journal of Controlled Release, 177*, 51–63.

Veronovski, A., Novak, Z., & Knez, Ž. (2012). Synthesis and use of organic biodegradable aerogels as drug carriers. *Journal of Biomaterials Science, Polymer Edition, 23*(7), 873–886.

Villegas, M., Oliveira, A. L., Bazito, R. C., & Vidinha, P. (2019). Development of an integrated one-pot process for the production and impregnation of starch aerogels in supercritical carbon dioxide. *The Journal of Supercritical Fluids, 154*, Article 104592.

Yahya, E. B., Alzalouk, M. M., Alfallous, K. A., & Abogmaza, A. F. (2020). Antibacterial cellulose-based aerogels for wound healing application: A review. *Biomedical Research and Therapy, 7*(10), 4032–4040.

Yu, X. X., Liu, Y. H., Liu, X. M., Wang, P. C., Liu, S., Miao, J. K., … Yang, C. X. (2018). Ascorbic acid induces global epigenetic reprogramming to promote meiotic maturation and developmental competence of porcine oocytes. *Scientific Reports, 8*(1), 6132.

Zhao, S., Malfait, W. J., Demilecamps, A., Zhang, Y., Brunner, S., Huber, L., … Koebel, M. M. (2015). Strong, thermally superinsulating biopolymer-silica aerogel hybrids by cogelation of silicic acid with pectin. *Angewandte Chemie, 127*(48), 14490–14494.

Zou, F., & Budtova, T. (2021). Tailoring the morphology and properties of starch aerogels and cryogels *via* starch source and process parameter. *Carbohydrate Polymers, 255*, Article 117344.